

Functional Display of Complex Cellulosomes on the Yeast Surface via Adaptive Assembly

Shen-Long Tsai,^{†,‡,§} Nancy A. DaSilva,^{||} and Wilfred Chen^{*,†}

[†]Department of Chemical and Biomolecular Engineering, University of Delaware, Newark, Delaware 19716, United States

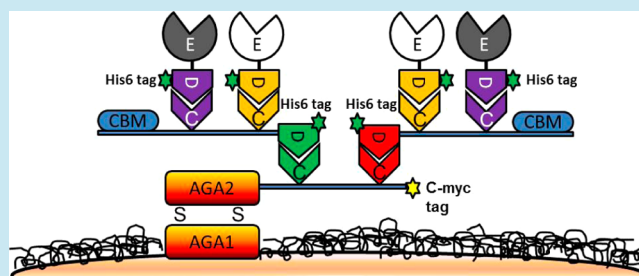
[‡]Department of Chemical and Environmental Engineering, University of California, Riverside, California 92521, United States

[§]Department of Chemical Engineering, National Taiwan University of Science and Technology, Taipei, Taiwan (R.O.C.)

^{||}Department of Chemical Engineering and Materials Science, University of California, Irvine, California 92697, United States

ABSTRACT: A new adaptive strategy was developed for the *ex vivo* assembly of a functional tetravalent designer cellulosome on the yeast cell surface. The design is based on the use of (1) a surface-bound anchoring scaffoldin composed of two divergent cohesin domains, (2) two dockerin-tagged adaptor scaffoldins to amplify the number of enzyme loading sites based on the specific dockerin–cohesin interaction with the anchoring scaffoldin, and (3) two dockerin-tagged enzymatic subunits (the endoglucanase Gt and the β -glucosidase Bglf) for cellulose hydrolysis. Cells displaying the tetravalent cellulosome on the surface exhibited a 4.2-fold enhancement in the hydrolysis of phosphoric acid swollen cellulose (PASC) compared with free enzymes. More importantly, cells displaying the tetravalent cellulosome also exhibited an \sim 2-fold increase in ethanol production compared with cells displaying a divalent cellulosome using a similar enzyme loading. These results clearly indicate the more crucial role of enzyme proximity than just simply increasing the enzyme loading on the overall cellulosomal synergy. To the best of our knowledge, this is the first report that exploits the natural adaptive assembly strategy in creating artificial cellulosome structures. The unique feature of the anchoring and the adaptor scaffoldin strategy to amplify the number of enzymatic subunits can be easily extended to more complex cellulosomal structures to achieve an even higher level of enzyme synergy.

KEYWORDS: cellulosome, yeast, scaffoldin, dockerin, cohesin, adaptor



Biofuels derived from lignocellulosic biomass are attractive alternatives to current petroleum-based fuels due to their sustainable and environment-friendly nature. However, the main technological obstacle to the more widespread use of this natural resource is the lack of a low-cost technology to overcome the source's recalcitrant nature, especially the hydrolysis of the highly ordered cellulose structure.¹ Improvements in the overall efficiency and yield of hydrolyzed sugars from lignocellulosic biomass have been pursued for several decades, including genetic engineering of crops for better sugar accessibility,² optimization of pretreatment technologies,³ and engineering cellulases for enhanced activity and stability.^{4,5} All of these efforts have resulted in improved sugar liberation from lignocellulosic biomass; however, the cost of extraneously added cellulases is still too prohibitively high to allow the more widespread replacement of petroleum-based fuels by lignocellulosic biofuels.

Many anaerobic bacteria have developed an elaborately structured multienzyme complex on the cell surface called the cellulosome for efficient cellulose hydrolysis.^{6,7} The main feature of the cellulosome is a structural scaffoldin consisting of at least one cellulose-binding module (CBM) and repeating cohesin domains, which are docked individually with different cellulases tagged with the corresponding dockerin domain.⁸

This highly ordered structure allows the assembly of multiple enzymes in close proximity, mediated by the high-affinity protein–protein interaction ($>10^{-9}$ M) between dockerin and cohesin, resulting in a high level of enzyme–substrate–microbe synergy toward cellulose and hemicellulose hydrolysis.

Because of the highly specific interaction between the dockerin and cohesin domain from the same species, chimeric scaffoldins composed of cohesins from three or four different species have been created, resulting in the formation of synthetic cellulosomes bearing the matching dockerin-tagged enzymes.^{9,10} Efforts have been made to display cellulosome structures on the yeast surface for cellulosic ethanol production.^{11–14} Our group has functionally displayed different mini-cellulosomes composed of three dockerin-tagged enzymes on the yeast surface either by *in vitro* assembly or by intercellular complementation using a synthetic yeast consortium,^{13,14} enabling simultaneous cellulose hydrolysis and ethanol production. Although the resulting engineered strains demonstrated up to 3-fold improvement in both the hydrolysis of phosphoric acid swollen cellulose (PASC) and subsequent

Received: May 18, 2012

Published: July 5, 2012

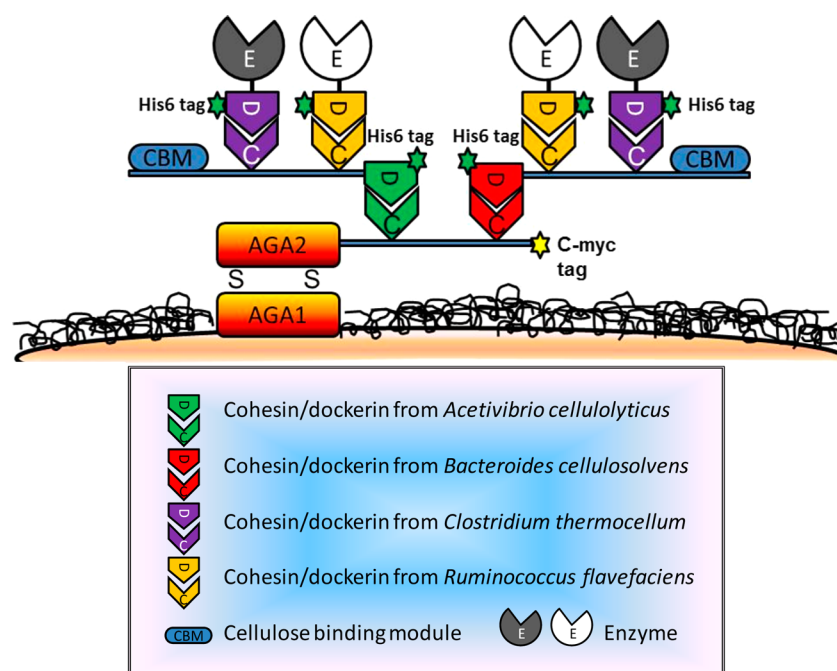


Figure 1. Schematic diagram of the complex cellulosome assembled on the yeast surface using the adaptive assembly. The two adaptor scaffoldins served as templates for enzyme recruitment to the yeast surface via specific interaction with the surface-displayed anchoring scaffoldin.

ethanol production when compared with free enzymes, any further improvement necessitates the assembly of more complex cellulosome structures as found in many naturally occurring cellulosomes. However, the creation of more complex artificial cellulosomes has not been realized probably due to the complexity of folding the larger chimeric scaffoldins.

Instead of employing a single scaffoldin and numerous dockerin-tagged enzymes for cellulosome formation as in the case of *Clostridium cellulovorans*¹⁵ and *Clostridium cellulolyticum*,¹⁶ some bacteria such as *Acetivibrio cellulolyticus*¹⁷ and *Bacteroides cellulosolvans*¹⁸ exhibit a more complex cellulosome structure, in which several adaptor scaffoldins were found in addition to a surface-displayed anchoring scaffoldin. These adaptor scaffoldins serve to amplify the number of enzymatic subunits that can be incorporated into the cellulosome complex and thereby effectively increase the overall enzyme density and hydrolytic efficiency.¹⁹

Inspired by this adaptive mechanism from nature, we report here the creation of a four-enzyme or tetravalent cellulosome structure on the yeast surface by mimicking the adaptor scaffoldin-mediated assembly strategy (Figure 1). Cells displaying the tetravalent cellulosome produced 2-fold more reducing sugars and ethanol from PASC compared with a mixture of cells displaying a two-enzyme or divalent cellulosome structure containing the same amount of enzymes.

RESULTS AND DISCUSSION

Design Strategy of Adaptive Assembly. We have previously displayed a trivalent cellulosome structure on the yeast surface suitable for cellulosic ethanol production. To further elevate the production rate, we sought to create a designer cellulosome with a higher enzyme density. Rather than simply extending the number of cohesin domains on the displayed scaffoldin, our design is based on an adaptive assembly strategy. This adaptive strategy was chosen primarily to avoid the improper folding problems encountered during the

display of complex scaffoldin structures containing more than three cohesin domains and to allow flexibility in synthesizing the different components for the assembly.

The initial design (Figure 1) is composed of an anchoring scaffoldin (AnScf) containing two divergent cohesin domains from *A. cellulolyticus* and *B. cellulosolvans*, respectively. These cohesin domains were functionally displayed on the yeast surface using the Aga1-Aga2 anchor.²⁰ A c-Myc tag was added to the C-terminus of the anchoring scaffoldin to allow for immuno-probing. To enable the display of a larger number of cohesin domains, two adaptor scaffoldins (AdpA and AdpB) containing a cellulose-binding module (CBM), the cohesin domain of *C. thermocellum* (t), the cohesin domain of *R. flavefaciens* (f), and either the dockerin domain of *A. cellulolyticus* or *B. cellulosolvans* at the C-terminus were constructed. A hexahistidine tag (his tag) was added to the C-terminus of each adaptor scaffoldin. By taking advantage of the specific interaction between the different dockerin/cohesin pairs, these adaptor scaffoldins can self-assemble onto the surface-bound AnScf and serve to amplify the number of enzymatic subunits in the resulting four-enzyme or tetravalent cellulosome structure. Finally, a recombinant endoglucanase CelG from *C. cellulolytica* tagged with the dockerin domain from *C. thermocellum* (Gt) and a β -glucosidase BglA from *C. thermocellum* tagged with the dockerin domain from *Ruminococcus flavefaciens* (Bglf) were used to enable the position-specific assembly of the two enzymes onto the adaptor scaffoldins. The possessive endoglucanase CelG was used in concert with the β -glucosidase in order to convert more than 50% of the released sugar oligomers to glucose as reported.²⁴

Functional Display of the Anchoring Scaffoldin on the Yeast Surface. To display the anchoring scaffoldin AnScf, the entire scaffold was fused to the Aga2p subunit of a-agglutinin²⁵ in a fashion similar to that used in our prior yeast display studies.¹³ The correct translocation of AnScf on the yeast surface was confirmed by immunofluorescence labeling using

the anti-c-Myc sera and Alexa 488 conjugated goat anti-mouse IgG. As shown in Figure 2, bright fluorescence was observed

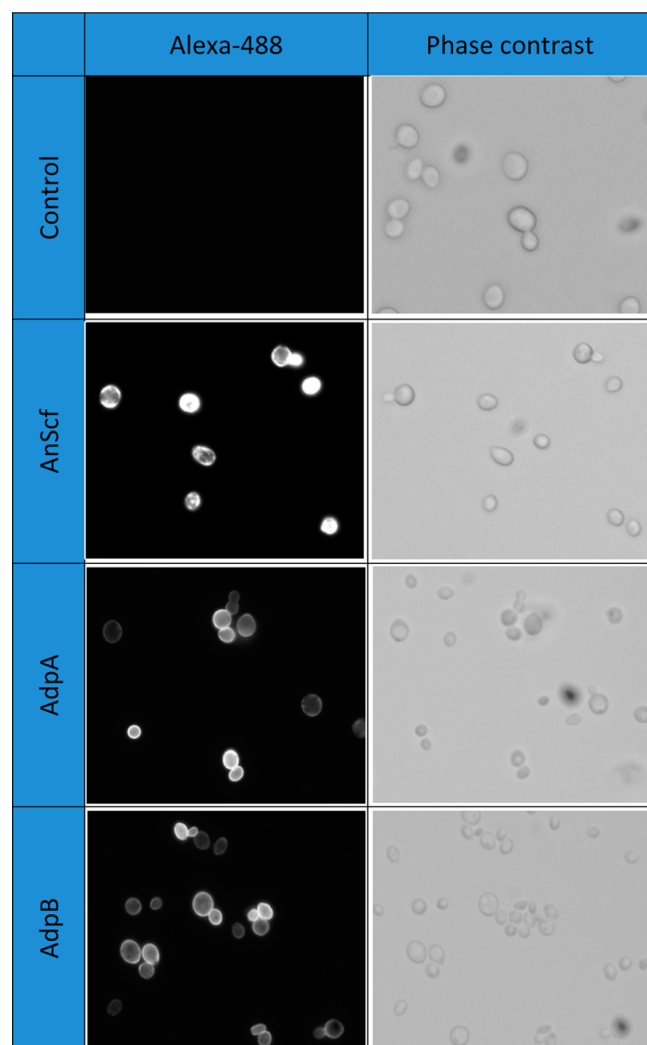


Figure 2. Phase-contrast and immunofluorescence micrographs of yeast cells displaying the anchoring scaffoldin (AnScf) and docked with the two adaptor scaffoldins (AdpA and AdpB). Cells were probed with either anti-C-myc sera (AnScf) or anti-C-His6 sera (AdpA and AdpB) and fluorescently stained with a goat anti-mouse IgG conjugated with Alexa Fluor 488. *S. cerevisiae* EBY100 was used as control.

with cells displaying AnScf, whereas no significant fluorescence was detected for the control cells. On average, a detectable fluorescence signal was observed for around 70% of the cells after induction, consistent with other reports using the Aga1-Aga2 anchor system for surface display.^{20,21,26}

Expression of the Adapter Scaffoldins and Their Functional Docking onto the Anchoring Scaffoldin.

The two adaptor scaffoldins were expressed in *E. coli* strain BL21 Gold under control of a strong T7 promoter. A strong band corresponding to the expected adaptor size was detected by SDS-PAGE for both cultures, although a major degraded protein band was also detected for AdpA (Figure 3A). However, expression of the full-length adaptors was confirmed by Western blot analysis by probing the C-terminus his tag (Figure 3B). Since the major degraded product of AdpA does not contain a functional his tag, this degraded product is

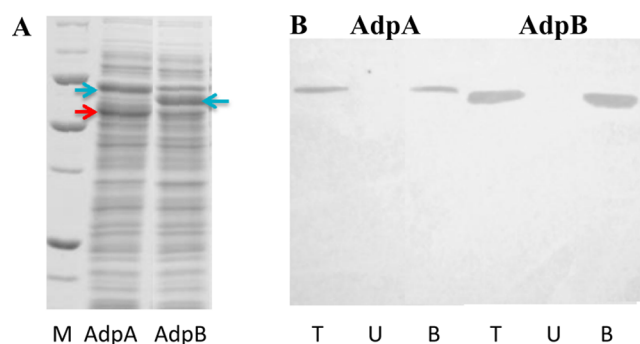


Figure 3. Expression and Avicel purification of adaptor scaffoldins confirmed by (A) 10% SDS-PAGE gel and (B) western-blot analysis. (A) M: protein marker; AdpA: cell lysate of AdpA; AdpB: cell lysate of AdpB. The full length AdpA and AdpB are indicated by a blue arrow, and the partially degraded AdpA is indicated by a red arrow. (B) T: total cell lysate, U: unbound fraction; B, bound fraction.

incapable of cohesin binding because the entire flanking dockerin domain is also degraded based on the size difference. On the other hand, the functionality of CBM on the full-length adaptors was demonstrated as both adaptors retained the ability to bind to Avicels (Figure 3B).²⁷

To test whether the adaptor scaffoldins could correctly associate with the surface displayed anchoring scaffoldin, additional immunofluorescence studies targeting the his tag epitope at the C-terminus of the adaptor scaffoldins were conducted. As expected, no significant fluorescence was detected with cells displaying AnScf. In contrast, a significant increase in the whole-cell fluorescence was detected when either one of the two adaptors was added to cells displaying AnScf, indicative of adaptor binding (Figure 4). More

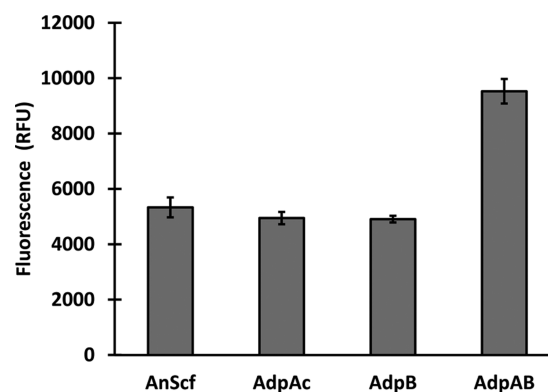


Figure 4. Surface assembly of adaptor scaffoldins was probed with either anti-C-myc sera for the anchoring scaffoldin (AnScf) or anti-C-His6 sera for the assembled adaptor scaffoldins (AdpA or AdpB) and fluorescently stained with a goat anti-mouse IgG conjugated with Alexa Fluor 488. Whole cell fluorescence was determined using a fluorescent microplate reader. Data shown are the mean values (\pm standard deviation) obtained from 3 independent experiments.

importantly, a similar level of fluorescence was detected from the c-Myc tag and his tag indicating the correct 1:1 binding between the anchoring and adaptor scaffoldin pairs. When these cells were further incubated with the other adaptor scaffoldin, an additive amount of fluorescence was detected (Figure 4). Taken together, these results indicated several important facts: (1) the two adaptor scaffoldins can successfully associate with the surface-displayed anchoring scaffoldin based

on the high-affinity cohesin-dockerin interaction; (2) there is no cross association between the two different dockerin-cohesin pairs since a comparable level of fluorescence was detected when only one adaptor was added; and (3) the steric hindrance between the two adaptor scaffoldins was negligible since a 2-fold increase in fluorescence was detected in the presence of a second adaptor scaffoldin.

Functional Assembly of the Complex Cellulosome.

After proving the functionality of the anchoring scaffoldins and the dockerin domains on the adaptors, the ability of the adaptor scaffoldins to recruit cellulases into a cellulosome structure through the specific dockerin-cohesin interaction was investigated. Cells displaying the anchoring scaffoldin were first saturated with either one or both adaptor scaffoldins as described above. *E. coli* lysates containing either the endoglucanase Gt or the β -glucosidase Bglf were then used for the enzyme assembly. Again, quantitative assessment of enzyme docking was performed by whole-cell immunofluorescence measurements by probing the C-terminus his tag of the adaptors and the enzymes. Binding of Gt to cells saturated with only one adaptor scaffoldin was confirmed by a 2-fold increase in the whole-cell fluorescence, independent of which adaptor was used for the assembly (Figure 5A). More importantly, an approximate 4-fold increase in the fluorescence intensity was observed when Gt was bound onto cells possessing both adaptor scaffoldins on their surface, indicating the successful assembly of Gt onto each adaptor. Similarly, the functionality of the *R. flavefaciens* cohesin in the two adaptors was confirmed by detecting the binding of Bglf. A 2- or 4-fold increase in the whole-cell fluorescence intensity was detected, respectively, when yeast cells possessing either one adaptor or two adaptors were used for Bglf docking (Figure 5B). Collectively, these results confirm the correct assembly of both enzymes onto the adaptor scaffoldins.

With the successful docking of each individual enzyme onto the adaptor scaffoldins, the feasibility of assembling both enzymes side by side onto the same adaptor was examined. Cells displaying AnScf were first saturated with the adaptor scaffoldin AdpA and the two enzymes Gt and Bglf. The correct assembly of the divalent cellulosome structure was confirmed by observing a 3-fold increase in the whole-cell fluorescence intensity after binding (Figure 5C). Finally, the complete assembly of the tetravalent cellulosome structure was performed by incubating AnScf-displaying cells with both adaptor scaffoldins and both enzymes. As shown in Figure 5C, a 2-fold further increase in the whole-cell fluorescence was detected compared with cells displaying only the divalent cellulosome structure, demonstrating the correct side-by-side assembly of both enzymes onto the two adaptor scaffoldins.

Synergistic Effects of the Complex Cellulosome. The synergistic effect on cellulose hydrolysis is the most intriguing property of naturally occurring cellulosomes and artificial cellulosomes.^{9,13,28} This can be attributed to either the direct substrate channeling, substrate targeting, and/or enzyme proximity effects.²⁹ To investigate the potential proximity effect even between the same set of two enzymes (the possessive endoglucanase Gt and the β -glucosidase Bglf), cellulose hydrolysis was compared by resting cells displaying different cellulosome structures (Figure 6). PASC, one of the most frequently used model substrates to evaluate the efficiency of cellulose hydrolysis, was used. In the first setup (S1), 50% of the yeast cells were docked with the two adaptor scaffoldins but no enzymes. The second setup (S2) contained 50% of the yeast

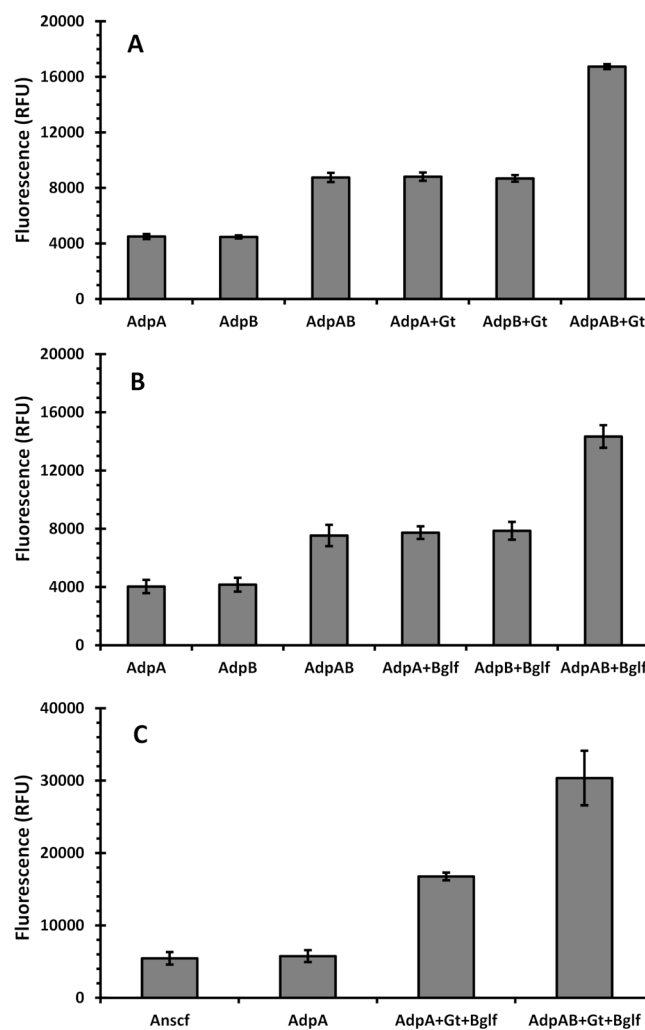


Figure 5. Surface assembly of (A) Gt, (B) Bglf, and (C) divalent or tetravalent cellulosomes was probed with either anti-C-myc sera for the anchoring scaffoldin or anti-C-His6 sera for the assembled adaptor scaffoldins and enzymes, followed by incubation with goat anti-mouse IgG conjugated with Alexa Fluor 488. Whole cell fluorescence was determined using a fluorescent microplate reader. Data shown are the mean values (\pm standard deviation) obtained from 3 independent experiments.

cells displaying a divalent cellulosome in which enzymes were recruited only to one adaptor (AdpA). In the third setup (S3), all cells displayed a divalent cellulosome, effectively doubling the bulk enzyme density as in S2. The last setup (S4) contained 50% of the yeast cells displaying a tetravalent cellulosome in which enzymes were recruited onto both adaptors (AdpA and AdpB); this setup provides the same enzyme density as in S3 except that all enzymes are presented in close proximity in the tetravalent cellulosome. Other than S3, the rest of the population was composed of cells displaying only the anchoring scaffoldin AnScf.

Figure 6A shows the time course of glucose released from PASC using the different cellulosome structures. Cells displaying the divalent cellulosome (S2) exhibited a significantly higher rate of glucose released than the control cells (S1). When the number of yeast cells displaying the divalent cellulosome was increased from 50% (S2) to 100% (S3), which corresponds to a 2-fold increase in the bulk enzyme density, a 2-fold increase in the glucose liberation was also observed. In

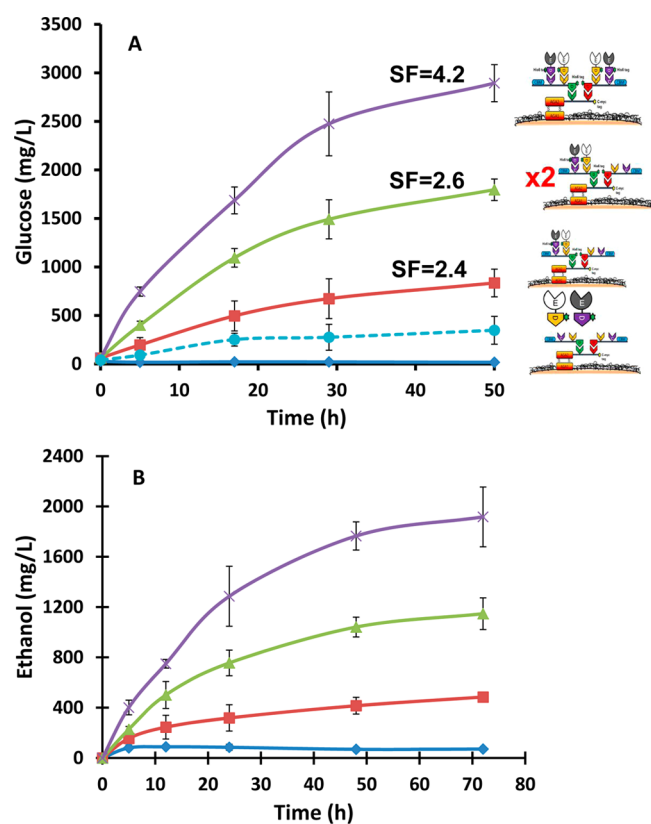


Figure 6. Production of glucose (A) and ethanol (B) from PASC using yeast cells displaying different cellulosome structures. (◆) S1, no enzymes; (■) S2, 50% cells composed of the divalent cellulosome; (▲) S3, 100% cells composed of the divalent cellulosome; (×) S4, 50% cells composed of the tetravalent cellulosome; (●) the same amount of free enzymes as in S2. Other than S3, the rest of the population was composed of cells displaying only the anchoring scaffoldin AnScf. The synergy factor (SF), cellulosome activity/free enzyme activity, for each cellulosome structure is listed.

comparison, cells displaying the tetravalent cellulosome (S4) exhibited a 1.6-fold further increase in the glucose production compared to S3. Since the same amount of enzymes was maintained in S3 and S4, this result clearly demonstrates that enzyme proximity, which results in enzyme co-localization, substrate channeling, and the cooperative action between enzymes, is much more important than the bulk enzyme density in improving cellulose hydrolysis.

To investigate how the different cellulosome structures affect the level of enzyme synergy (glucose released from the cellulosome structure over glucose released from free enzymes), PASC hydrolysis was compared with a similar amount of free enzymes (both Gt and Bglf) as in S2. As shown in Figure 6A, the level of synergy increased from 2.4 (S2) to 2.6 (S3) for the divalent cellulosome structures to 4.2 (S4) for the tetravalent cellulosome structure. It is interesting to note that the level of synergy did not change for the divalent cellulosome structure even at a 2-fold higher enzyme loading (S3). This result clearly confirms the benefit of using a more complex cellulosome structure in enhancing cellulose hydrolysis.

Direct Fermentation of Amorphous Cellulose to Ethanol. The level of ethanol production from PASC was compared among the different cellulosome structures in resting-cell fermentation. While glucose inhibition of β -glucosidase is well documented in resting cell experi-

ments,^{13,30,31} this inhibition can be eliminated by the quick glucose uptake during fermentation. As shown in Figure 6B, the level of ethanol production was well correlated to the trend observed in the resting-cell cellulose hydrolysis experiment. The maximum ethanol production for S4 was 1.9 g/L after 72 h. Moreover, no detectable glucose accumulation in the medium was observed, indicating the quick uptake of glucose. The level of ethanol production for S3 was 1.7-fold lower than S4, consistent with the resting-cell hydrolysis experiment. More importantly, the higher level of enzyme synergy afforded by the tetravalent cellulosomal design resulted in more than 4-fold improvement in the ethanol production when compared to the divalent structure in S2 even though the enzyme density was increased only 2-fold. This nonlinear scaling in enzyme synergy provided by enzyme clustering is perhaps the main reason why natural cellulosomes are all multivalent by design.³² It is clear that the more practical utility of synthetic cellulosomes is to harness the nonlinear nature of the enzyme synergy by increasing the overall enzyme density and proximity via the formation of more complex cellulosomes.

Discussion. Although mini-cellulosome structures have been assembled^{9,10} or displayed onto the surface of microbes,^{21,32–34} artificial cellulosomes containing more than four enzymes have not been successfully created. This is likely due to the improper folding of the large chimeric structures containing a larger number of cohesin domains from different species. Inspired by the adaptive strategy employed by nature to assemble complex cellulosomes, the long-term goal of this work is to demonstrate the use of synthetic anchoring and adaptor scaffoldins to display more complex cellulosome structures. To our best knowledge, this is the first report that exploits the natural adaptive assembly strategy into artificial cellulosome structures.

Specifically, we presented here the feasibility of assembling a tetravalent cellulosome on the yeast surface using this anchoring/adaptor scaffoldin-mediated assembly strategy. In this design, a divalent anchoring scaffoldin was displayed on the yeast surface to recruit two adaptor scaffoldins based on the strong and specific interaction between the matching cohesin/dockerin pairs. The engineered yeasts possessing the complete tetravalent cellulosome on the surface exhibited a 4-fold increase in ethanol production over those displaying a divalent cellulosome, indicating the crucial role of enzyme proximity on the cellulosomal synergy. This result demonstrates that the cooperative action even between the same two endoglucanase Gt and β -glucosidase Bglf can be significantly promoted by their integration into a single tetravalent cellulosome structure. It is difficult to assess the complete benefit on ethanol production since the tetravalent cellulosome assembled here lacks a functional exoglucanase and not all of the hydrolyzed PASC can be converted to glucose and subsequently to ethanol. However, considering the more than 2-fold improvement even with the two-enzyme system employed, we fully expect that a higher level of improvement can be achieved when a larger number of enzymes are incorporated. This has been illustrated recently by showing that an *in vitro* reconstituted CipA cellulosome structure containing nine enzymes has ~4-fold higher activity when compared with that of a mini-cellulosome containing only three enzymes.³⁵

The unique feature of the anchoring and the adaptor scaffoldin strategy to amplify the number of enzymatic subunits can be easily extended to more complex cellulosomal structures by using additional adaptor scaffoldins in order to achieve a

higher level of enzyme synergy. Since we have already demonstrated that a synthetic yeast consortium secreting different cellulases can be engineered to assemble a fully functional mini-cellulosome on the yeast surface, we envision that the consortium strategy can be similarly employed to secrete the adaptors for assembly. This adaptive strategy is particularly well suited for our consortium design in displaying more complex cellulosome structures because of the flexibility in producing the required anchoring and adaptor scaffoldins for the complex assembly. However, given the complexity of the different populations involved in the consortium, this will require very detailed coordination of the different yeast populations in order to maintain the overall functionality.

In conclusion, this work has successfully demonstrated the concept of using an adaptive strategy for the display of complex cellulosomes and the importance of enzyme proximity on enhanced cellulose hydrolysis.

METHODS

Strains and Media. *Escherichia coli* strain JM109 [*endA1*, *recA1*, *gyrA96*, *thi*, *hsdR17* (r_k^- , m_k^+), *relA1*, *supE44*, Δ (*lac-proAB*)] was used as the host for genetic manipulations. *E. coli* strains BL21 (DE3) [F^- *ompT gal hsdS_B* ($rB^- mB^-$) *dcm lon* λ DE3] and BL21-Gold (DE3) [F^- *ompT gal hsdS_B* ($rB^- mB^-$) *dcm lon* λ DE3] were used as production hosts for cellulases and adaptors expression. *Saccharomyces cerevisiae* strain EBY100 [*MATa AGA1::GAL1-AGA1::URA3 ura3-52 trp1 leu2_1 his3_200 pep4::HIS3 prb1_1.6R can1 GAL*] was used for surface display of the anchoring scaffoldin. All *E. coli* cultures were grown in Luria–Bertani (LB) medium (10.0 g/L tryptone, 5.0 g/L yeast extract, 10.0 g/L NaCl), supplemented with either 100 μ g/mL ampicillin or 50 μ g/mL karamycin. All yeast cultures were grown in SDC medium (20.0 g/L dextrose, 6.7 g/L yeast nitrogen base without amino acids, 5.0 g/L casamino acids).

Plasmid Construction. The gene fragments coding for the cohesin and dockerin domains of either *A. cellulolyticus* (Genbank Accession No. AF155197) or *B. cellulosolvans* (Genbank Accession No. AF224509) were purchased from GenScript (Piscataway, NJ, USA). To display the anchoring scaffoldin, fragments coding for the two cohesin domains were digested with *NdeI* and *Sall* and ligated into plasmid pCTCON2²⁰ to create an in-frame C-terminal fusion to the AGA2 gene. The resulting plasmid pCohAcBc was under the control of a galactose-inducible promoter and flanked with a *C-myc* tag at the C-terminus, which facilitates the confirmation of protein translocation via immunofluorescence microscopy.

The adaptor scaffoldins were constructed as follows. The gene fragments for the dockerin domains were first digested with *SacI* and *NotI*. The resulting fragments were separately cloned into the same sites of the expression vector pET24a to generate pDockAc and pDockBc. The sequence coding for the cohesin domain from *Ruminococcus flavefaciens*, the cohesin domain from *C. thermocellum*, and the cellulose binding module (CBM) was obtained using plasmid YCplac33-AG α -scaf3²¹ as the template by PCR amplification using the forward primer F2Coh1CBM (5'-GCTAGCTAGCGCTACGGCTACGCC-3') and the reverse primer R2Coh1CBM (5'-GCTA-GAGTCCTTAACAATGATAGCGCCAT-3'). The PCR product was further digested and ligated into the *NheI* and *SacI* sites of pDockAc and pDockBc to form pETAdpA and pETAdpB.

The recombinant endoglucanase (Gt) was constructed by fusing the endoglucanase CelG from *C. cellulolyticum* with the dockerin from *C. thermocellum* as described below. The catalytic domain of CelG was amplified by PCR using pETGt¹¹ as the template using primers F CelG (5'-GCTAGCTAGCGGAACA-TATAACTATGGA-GAAGCATTACAG-3') and R CelG (5'-GCATGCGGCCGCAGGAACGAGCT-TTGTGC-3'). The PCR product was then digested with *NheI* and *NotI* and ligated into the same restriction sites of plasmid pET24a to generate pETCelG Δ Dock. The dockerin from *C. thermocellum* was obtained by PCR using pETAt¹³ as the template with primers F DockCt (5'-GCTAGCGGCCGCAACTTC-CCGAATCCTTTGAGTGAC-3') and R DockCt (5'-GCTACTCGAGATAAGGTAGGTGGGGTATGC-3'). The resulting fragment was further digested with *NotI* and *XhoI* and cloned into pETCelG Δ Dock to form pETGt. The construction of plasmid pBglAf encoding a β -glucosidase from *C. thermocellum* and a dockerin domain from *R. flavesfaciens* was described elsewhere.¹³

Display of Anchor Protein on Yeast Surface. For the display of anchoring scaffoldin on the yeast surface, yeast cells harboring pCohAcBc were precultured in SDC medium for 18 h at 30 °C. These precultures were further washed with SGC medium (20.0 g/L galactose, 6.7 g/L yeast nitrogen base without amino acids, 5.0 g/L casamino acids) once and then subinoculated into 200 mL of SGC medium at an optical density (OD₆₀₀) of 0.5 and grown for 48 h at 20 °C.

Expression of Adaptor Scaffoldins and Dockerin-Tagged Cellulases. *E. coli* BL21 (DE3) strains expressing the adaptor scaffoldins AdpA and AdpB, and the recombinant β -glucosidase BglAf were precultured overnight at 37 °C in LB medium supplemented with appropriate antibiotics. The precultures were subinoculated in 200 mL LB medium supplemented with 1.5% glycerol and appropriate antibiotics at an initial OD of 0.01 and incubated at 37 °C until the O.D. reached 1.5. The cultures were then cooled to 20 °C, and isopropyl thio- β -D-galactoside (IPTG) was added to a final concentration of 100 μ M. After 16 h, cells were harvested by centrifugation (3000 \times g, 10 min) at 4 °C, resuspended in buffer A (50 mM Tris-HCl pH 8.0, 100 mM NaCl, and 10 mM CaCl₂), and lysed with a sonicator. A similar procedure was used for expressing the recombinant endoglucanase Gt except that the *E. coli* strain BL21-Gold (DE3) was used.

To confirm the proper folding of both adaptors, we further investigated the amenability of the resultant hybrid proteins for affinity-purification on cellulose via their CBM. This purification procedure could be accomplished by batch adsorption to and desorption from cellulose matrices.

Assembly of Complex Cellulosome of the Yeast Surface. To assemble the cellulosomes, cell lysates containing either one or both of the adaptor scaffoldins were incubated with yeast cells displaying the anchoring scaffoldin for 1 h at 4 °C in buffer A. After incubation, cells were washed and harvested by centrifugation (3000 \times g, 10 min) at 4 °C and resuspended in the same buffer with a higher adaptor concentration. Similar experiments with increasing adaptor concentrations were repeated in order to saturate all the cohesin domains in the anchoring scaffoldin. Thereafter, yeast cells saturated with adaptors were incubated with cell lysates containing either CelGt or BglAf for 1 h at 4 °C in buffer A as above.

Immunofluorescence Microscopy. Immunofluorescence microscopy and whole cell fluorescence measurements were

performed as described.¹³ Yeast cells displaying either the anchoring scaffoldin, the adaptor scaffoldin, and/or enzymes were harvested by centrifugation, washed with PBS buffer (8 g/L NaCl, 0.2 g/L KCl, 1.44 g/L Na₂HPO₄, 0.24 g/L KH₂PO₄), and resuspended in 250 μ L of PBS buffer containing 1 mg/mL BSA and 0.5 μ g of anti-C-Myc or anti-C-His IgG (Applied Biological Materials Inc.) for 2 h with occasional mixing. Cells were then pelleted and washed with PBS before resuspending in PBS buffer plus 1 mg/mL BSA and 0.5 μ g of anti-mouse IgG conjugated with Alexa 488 (Molecular Probes). After incubating for 1 h, cells were pelleted and washed twice with PBS, followed by resuspension in PBS buffer to an OD₆₀₀ of 1. For fluorescence microscopy (Olympus BX51), 5–10 μ L of cell suspensions were spotted on slides and a coverslip was added. Images from Alexa 488 were captured using the QCapture Pro6 software. Whole cell fluorescence was measured using a fluorescent microplate reader (Synergy4, BioTek, VT) with an excitation wavelength at 485 nm and an emission wavelength at 535 nm.

Enzyme Assays. Carboxymethyl cellulose (CMC) was obtained from Sigma and used as a substrate. Phosphoric acid swollen cellulose (PASC) was prepared from Avicel PH101 (Sigma) according to the method of Walseth.²² Enzyme activity was assayed in the presence of a 0.3% (w/v) concentration of cellulose at 30 °C in 20 mM Tris-HCl buffer (pH 6.0). Samples were collected periodically and immediately mixed with 3 mL of DNS reagents (10 g/L dinitrosalicylic acid, 10 g/L sodium hydroxide, 2 g/L phenol, 0.5 g/L sodium sulfite). After incubating at 95 °C for 10 min, 1 mL of 40% Rochelle salts was added to fix the color before measuring the absorbance of the supernatants at 575 nm. Glucose concentration was determined using a glucose HK assay kit from Teco Diagnostic (Anaheim, California, USA).

Fermentation. Anaerobic fermentation was conducted at 30 °C in 10-mL rubber-stoppered glass serum bottles. Briefly, yeast cells were washed once with buffer containing 50 mM Tris-HCl, pH 8.0, 100 mM NaCl, and 10 mM CaCl₂ and resuspended in SDC medium containing 6.7 g/L yeast nitrogen base without amino acids, 20 g/L casamino acids, and 10 g/L PASC as the sole carbon source. Reducing sugars and glucose concentration were measured by the methods described above. The amount of residual cellulose was measured by the phenol-sulfuric acid method as described by Dubois et al.²³ Ethanol concentration was measured by gas chromatography (model 7890, Agilent, USA) using a flame ionization detector and HP-5 column.

AUTHOR INFORMATION

Corresponding Author

*Tel: (302) 831-6327. E-mail: wilfred@udel.edu.

Notes

The authors declare no competing financial interest.

ACKNOWLEDGMENTS

This research was supported by grants from NSF (CBET 0903894) and DOE (EE0000988).

REFERENCES

(1) Lynd, L. R., Weimer, P. J., van Zyl, W. H., and Pretorius, I. S. (2002) Microbial cellulose utilization: fundamentals and biotechnol-ogy. *Microbiol. Mol. Biol. Rev.* 66, 506–577.

(2) Hisano, H., Nandakumar, R., and Wang, Z. Y. (2009) Genetic modification of lignin biosynthesis for improved biofuel production. *In Vitro Cell. Dev. Biol.: Plant* 45, 306–313.

(3) Studer, M. H., DeMartini, J. D., Brethauer, S., McKenzie, H. L., and Wyman, C. E. (2010) Engineering of a high-throughput screening system to identify cellulosic biomass, pretreatments, and enzyme formulations that enhance sugar release. *Biotechnol. Bioeng.* 105, 231–238.

(4) Hardiman, E., Gibbs, M., Reeves, R., and Bergquist, P. (2010) Directed evolution of a thermophilic beta-glucosidase for cellulosic bioethanol production. *Appl. Biochem. Biotechnol.* 161, 301–312.

(5) Li, Y. C., Irwin, D. C., and Wilson, D. B. (2010) Increased crystalline cellulose activity via combinations of amino acid changes in the family 9 catalytic domains and family 3c cellulose binding module of *Thermobifida fusca* Cel9A. *Appl. Environ. Microbiol.* 76, 2582–2588.

(6) Bayer, E. A., Belaich, J. -P., Shoham, Y., and Lamed, R. (2004) The cellulosomes: Multienzyme machines for degradation of plant cell wall polysaccharides. *Annu. Rev. Microbiol.* 58, 521–554.

(7) Doi, R. H., and Kosugi, A. (2004) Cellulosomes: Plant-cell-wall-degrading enzyme complexes. *Nat. Rev. Microbiol.* 2, 541–551.

(8) Shoham, Y., Lamed, R., and Bayer, E. A. (1999) The cellulosome concept as an efficient microbial strategy for the degradation of insoluble polysaccharides. *Trends Microbiol.* 7, 275–281.

(9) Fierobe, H. P., Mingardon, F., Mechaly, A., Belaich, A., Rincon, M. T., Pages, S., Lamed, R., Tardif, C., Belaich, J. P., and Bayer, E. A. (2005) Action of designer cellulosomes on homogeneous versus complex substrates: Controlled incorporation of three distinct enzymes into a defined trifunctional scaffoldin. *J. Biol. Chem.* 280, 16325–16334.

(10) Morais, S., Barak, Y., Caspi, J., Hadar, Y., Lamed, R., Shoham, Y., Wilson, D. B., and Bayer, E. D. (2010) Cellulase-xylanase synergy in designer cellulosomes for enhanced degradation of a complex cellulosic substrate. *MBio* 1 (5), No. e00285-10.

(11) Wen, F., Sun, J., and Zhao, H. M. (2010) Yeast surface display of trifunctional minicellulosomes for simultaneous and synergistic saccharification and fermentation of cellulose to ethanol. *Appl. Environ. Microbiol.* 76, 1251–1260.

(12) Ito, J., Kosugi, A., Tanaka, T., Kuroda, K., Shibasaki, S., Ogino, C., Ueda, M., Fukuda, H., Doi, R. H., and Kondo, A. (2009) Regulation of the display ratio of enzymes on the *Saccharomyces cerevisiae* cell surface by the immunoglobulin G and cellulosomal enzyme binding domains. *Appl. Environ. Microbiol.* 75, 4149–4154.

(13) Tsai, S. -L., Oh, J., Singh, S., Chen, R. Z., and Chen, W. (2009) Functional assembly of minicellulosomes on the *Saccharomyces cerevisiae* cell surface for cellulose hydrolysis and ethanol production. *Appl. Environ. Microbiol.* 75, 6087–6093.

(14) Tsai, S. L., Goyal, G., and Chen, W. (2010) Surface display of a functional minicellulosome by intracellular complementation using a synthetic yeast consortium and its application to cellulose hydrolysis and ethanol production. *Appl. Environ. Microbiol.* 76, 7514–7520.

(15) Shoseyov, O., and Doi, R. H. (1990) Essential 170-kDa subunit for degradation of crystalline cellulose by *Clostridium cellulovorans* cellulase. *Proc. Natl. Acad. Sci. U.S.A.* 87, 2192–2195.

(16) Faure, E., Belaich, A., Bagnara, C., Gaudin, C., and Belaich, J. -P. (1989) Sequence analysis of the *Clostridium cellulolyticum* endoglucanase-A-encoding gene, *celCCA*. *Gene* 84, 39–46.

(17) Xu, Q., Gao, W., Ding, S. -Y., Kenig, R., Shoham, Y., and Bayer, E. A. (2003) The cellulosome system of *Acetivibrio cellulolyticus* includes a novel type of adaptor protein and a cell-surface anchoring protein. *J. Bacteriol.* 185, 4548–4557.

(18) Ding, S. -Y., Bayer, E. A., Steiner, D., Shoham, Y., and Lamed, R. (2000) A scaffoldin of the *Bacteroides cellulosolvens* cellulosome that contains 11 type II cohesins. *J. Bacteriol.* 182, 4915–4925.

(19) Fontes, C. M. G. A., and Gilbert, H. J. (2010) Cellulosomes: Highly efficient nanomachines designed to deconstruct plant cell wall complex carbohydrates. *Annu. Rev. Biochem.* 79, 655–681.

(20) Boder, E. T., and Wittrup, K. D. (1997) Yeast surface display for screening combinatorial polypeptide libraries. *Nat. Biotechnol.* 15, 553–557.

- (21) Goyal, G., Tsai, S. -L., Da Silva, N., and Chen, W. (2011) Simultaneous cell growth and ethanol production from cellulose by an engineered yeast consortium displaying a functional mini-cellulosome. *Microb. Cell Fact.* 10, 89 DOI: 10.1186/1475-2859-10-89.
- (22) Walseth, C. S. (1952) Occurrence of cellulases in enzyme preparations from microorganisms. *TAPPI J.* 35, 228–233.
- (23) Dubois, M., Gilles, K. A., Hamilton, J. K., Rebers, P. A., and Smith, F. (1956) Colorimetric method for determination of sugars and related substances. *Anal. Chem.* 28, 350–356.
- (24) Gal, L., Gaudin, C., Belaich, A., Pages, S., Tardif, C., and Belaich, J. -P. (1997) CelG from *Clostridium cellulolyticum*: a mutidomain endoglucanase acting efficiently on crystalline cellulose. *J. Bacteriol.* 179, 6595–6601.
- (25) Shen, Z. M., Wang, L., Pike, J., Jue, C. K., Zhao, H., de Nobel, H., Kurjan, J., and Lipke, P. N. (2001) Delineation of functional regions within the subunits of the *Saccharomyces cerevisiae* cell adhesion molecule a-agglutinin. *J. Biol. Chem.* 276, 15768–75.
- (26) Keike, M. C., Cho, B. K., Boder, E. T., Kranz, D. M., and Wittrup, K. D. (1997) Isolation of anti-T cell receptor scFv mutants by yeast surface display. *Protein Eng.* 10, 1303–1310.
- (27) Barak, Y., Handelsman, T., Nakar, D., Mechaly, A., Lamed, R., Shoham, Y., and Bayer, E. A. (2005) Matching fusion protein systems for affinity analysis of two interacting families of protein: the cohesin-dockerin interaction. *J. Mol. Recognit.* 18, 491–501.
- (28) Lu, Y. P., Zhang, Y. H. P., and Lynd, L. R. (2006) Enzyme-microbe synergy during cellulose hydrolysis by *Clostridium thermocellum*. *Proc. Natl. Acad. Sci. U.S.A.* 103, 16165–16169.
- (29) Bayer, E. A., Lamed, R., and Himmel, M. E. (2007) The potential of cellulases and cellulosomes for cellulosic waste management. *Curr. Opin. Biotechnol.* 18, 1–9.
- (30) Wong, D. W. S. (1995) *Food Enzymes: Structure and Mechanisms*, 1st ed., Springer, New York.
- (31) Demain, A. L., Newcomb, M., and Wu, J. H. D. (2005) Cellulase, clostridia, and ethanol. *Microbiol. Mol. Biol. Rev.* 69, 124–154.
- (32) Bayer, E. A., Henrissat, B., and Lamed, R. (2008) The cellulosome: A natural bacterial strategy to combat biomass recalcitrance, in *Biomass Recalcitrance* (Himmel, M. E., Ed.) pp 407–426, Blackwell, London.
- (33) Anderson, T. D., Robson, S. A., Jiang, X. W., Malmirchegini, G. R., Fierobe, H. P., Lazazzera, B. A., and Clubb, R. T. (2011) Assembly of Minicellulosomes on the Surface of *Bacillus subtilis*. *Appl. Environ. Microbiol.* 77, 4849–4858.
- (34) Wieczorek, A. S., and Martin, V. J. J. (2010) Engineering the cell surface display of cohesins for assembly of cellulosome-inspired enzyme complexes on *Lactococcus lactis*. *Microb. Cell Fact.* 9, 69.
- (35) Krauss, J., Zverlov, V. V., and Schwarza, W. H. (2012) *In vitro* reconstitution of the complete *Clostridium thermocellum* cellulosome and synergistic activity on crystalline cellulose. *Appl. Environ. Microbiol.* 78, 4301–4307.